Provided for non-commercial research and educational use only.
Not for reproduction or distribution or commercial use.

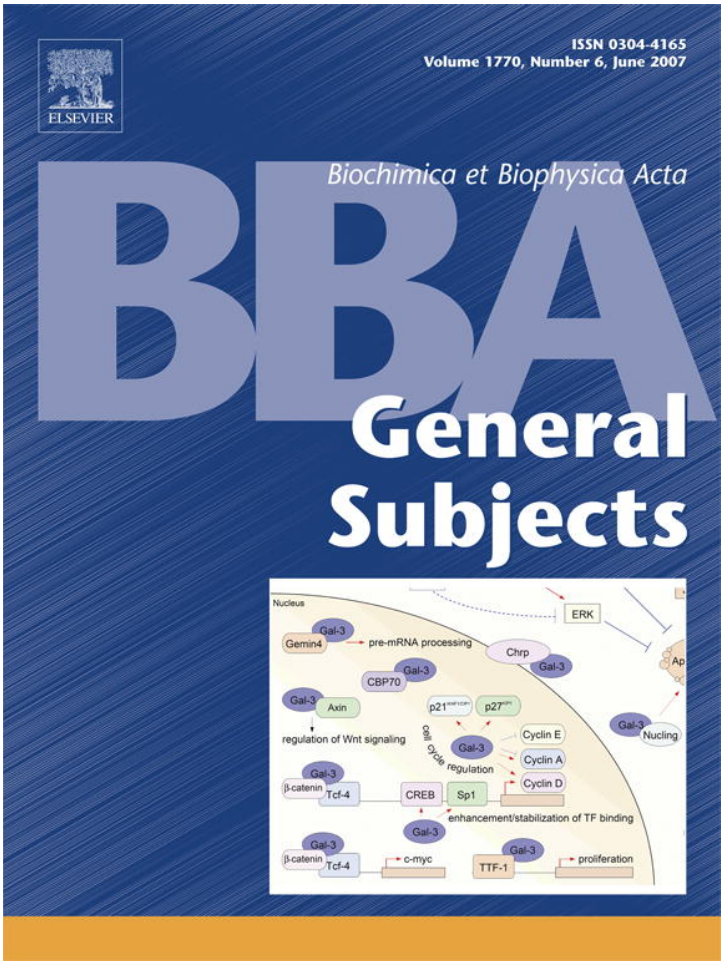
ISSN 0304-4165
Volume 1770, Number 6, June 2007
ELSEVIER
Biochimica et Biophysica Acta
BBA
General
Subjects

This article was originally published in a journal published by Elsevier, and the attached copy is provided by Elsevier for the author's benefit and for the benefit of the author's institution, for non-commercial research and educational use including without limitation use in instruction at your institution, sending it to specific colleagues that you know, and providing a copy to your institution's administrator.

All other uses, reproduction and distribution, including without limitation commercial reprints, selling or licensing copies or access, or posting on open internet sites, your personal or institution's website or repository, are prohibited. For exceptions, permission may be sought for such use through Elsevier's permissions site at:

http://www.elsevier.com/locate/permissionusematerial

Available online at www.sciencedirect.com
ScienceDirect
Biochimica et Biophysica Acta 1770 (2007) 912–918
Biochimica et Biophysica Acta
BBA
www.elsevier.com/locate/bbagen

Feasibility study using surface-enhanced Raman spectroscopy for the quantitative detection of tyrosine and serine phosphorylation

J. Moger [a,*], P. Gribbon [b,1], A. Sewing [b], C.P. Winlove [a]

[a] *School of Physics, University of Exeter, Stocker Road, Exeter, EX4 4QL, UK*
[b] *Pfizer Global Research and Development, Sandwich Laboratories, Ramsgate Road, Sandwich, Kent, CT13 9NJ, UK*

Received 19 September 2006; received in revised form 5 January 2007; accepted 31 January 2007
Available online 12 February 2007

Abstract

We investigate the feasibility of colloid-based surface enhanced Raman scattering (SERS) as a highly sensitive technique for detecting peptide phosphorylation at serine and tyrosine residues. Using the recently reported drop-coating deposition Raman method we validate our SERS spectra against normal Raman spectra that would otherwise be unobtainable at such low concentrations. Compared with existing techniques for quantifying peptide phosphorylation, such as high-performance liquid chromatography (HPLC), the short scanning and processing time associated with SERS makes it an attractive alternative for near-real-time measurement at sub micro-molar concentrations. Following pre-processing by Savistky–Golay second derivative (SGSD), the degree of phosphorylation of synthetic peptides is determined using multivariate spectral classification, interval partial least squares (iPLS). Furthermore, our results show that the technique is robust to interference from complex proteins and other phosphorylated compounds present at concentrations typically found in a screening assay.
© 2007 Elsevier B.V. All rights reserved.

Keywords: Surface enhanced Raman scattering; Peptide; Phosphorylation; Serine; Tyrosine

1. Introduction

Protein phosphorylation is intimately involved in numerous biological processes such as signal transduction [1], cell cycle control [2], immune response [3] and in the aetiology of diseases such as cancer and atherosclerosis [4]. The kinase family now comfortably exceeds 500 members, with at least 35 having clinical relevance as targets for drug discovery [5]. Therefore, sensitive detection of phosphorylation events is key to the identification of modulators of kinase activity [6]. Current kinase screening 'platform' technologies now include AlphaScreen (Perkin Elmer), IMAP beads (Molecular Devices), antibody based detection (Invitrogen) and Electrophoretic separation (Caliper Lifesciences). All of the techniques have advantages and disadvantages in terms of sensitivity, dynamic range and cost, but new techniques to quantify kinase activity are constantly evolving. In this publication we present a further addition to the portfolio of analytical methods, in the form of direct assessment of peptide phosphorylation based on surface enhance Raman spectroscopy (SERS).

Raman spectroscopy is a well-established technique for structural analysis of proteins and amino acids with applications ranging from forensics to the food industry [7–10]. However, the low scattering cross-section associated with Raman methods restricts its intrinsic sensitivity; typically analyte concentrations of 50 μM are required with extended sample readout times [11]. Recently, drop coating deposition Raman (DCDR) [12–15] has extended the working range down to 1 μM. In DCDR low volumes (~5 μl) are dried on a hydrophobic surface and evaporation effects give rise to a concentrated solid-like state which is reported to display essentially identical spectral features to dilute solution measurements [12]. However, integration times remain of the order of 10^2 s, which is incompatible with the timescale of applications such as High Throughput Screening (HTS). SERS combines Raman spectroscopy with the exciting properties of metallic nanostructures resulting in a vast amplification of the Raman signal, as high as

---

* Corresponding author.
E-mail address: j.moger@ex.ac.uk (J. Moger).

[1] Current Address: GlaxoSmithKline Research and Development Limited, Medicines Research Centre, Gunnels Wood Road, Stevenage, Herts SG1 2NY.

0304-4165/$ - see front matter © 2007 Elsevier B.V. All rights reserved.
doi:10.1016/j.bbagen.2007.01.018

14 orders of magnitude, when molecules are absorbed onto specific ‘SERS-active’ metallic nanometre-scale structures. Previously SERS has been used to analyse excitatory amino acids [16], neurotransmitters [17], DNA [18,19] and in living cells [20]. The most common types of SERS-active substrates, exhibiting the greatest enhancements ($>10^{12}$), are solutions of colloidal gold and silver particles in the 10–100 nm size range [21–24]. Other common SERS-active substrates include roughened metallic electrode surfaces [25–28], silver and gold nano-particle arrays [29–31], and so-called SERS optical fibre probes, where the end of an optical fibre is covered by a SERS-active surface [32–34].

In this study, we employed colloidal silver as a SERS substrate to detect phosphorylation of synthetic peptides at tyrosine and serine residues. Colloidal substrates have great potential for future application in HTS due to their high enhancement factors allowing rapid readout times, their compatibility with automated liquid handling, and low cost for large scale analysis. The enhancement of the Raman signal is mediated by the excitation of surface plasmons on the colloid surface which produce localised concentrated electromagnetic fields often referred to as ‘hot-spots’ [35]. The compatibility of our colloid with the excitation wavelength used was assessed via measurement of the surface plasmon resonance (SPR), which also served to confirm the origin of the enhancement. Extinction spectra of the colloid were obtained both before and after the addition of the analyte and the features analysed to confirm the shift in SPR.

The low solubility of the peptides prevented the acquisition of normal Raman spectra, therefore, our enhanced spectra are validated against those obtained using drop-coating deposition Raman (DCDR). With the aid of interval partial least squares (iPLS) multivariate analysis, we show that SERS can be used to quantify the degree of phosphorylation in a peptide mixture at biologically useful concentrations. Finally, the stability of the technique to interference from species such as proteins and other phosphate containing biomolecules that would be present in a ‘real-life’ screening assay is tested. Assay conditions were simulated by the addition of bovine serum albumin (BSA), adenosine diphosphate (ADP) and adenosine triphosphate (ATP) to the synthetic peptides prior to acquisition of SERS spectra and subsequent multivariant analysis.

2. Materials and methods

The synthetic peptides used in this study were purchased from PEPCEUTICALS LTD (Nottingham, UK), with purity 99% ascertained by HPLC. Peptides were either non-phosphorylated or singly phosphorylated at a serine and tyrosine residue (see sequences in Table 1). Aqueous solutions of each peptide were prepared at 100 μM in ultra-pure water (Purite, Oxford, UK); these were subsequently mixed in the correct fractions to produce 100 μM solutions with phosphorylated to non-phosphorylated peptide ratios ranging from 1 to 10%. Silver colloid was prepared by adding $AgNO_3$ (1 mM), drop-wise to $NaBH_4$ (2 mM) under constant stirring at 25 °C (pH 5.5 to 6). The $AgNO_3$ stock was stored under dark conditions and used within 1 h of preparation. Colloids were used within 10 min of preparation to ensure signal stability [21]. All reagents were Analar grade (SIGMA-ALDRICH, Poole, UK), and all water used was ultra-pure (PURITE, Oxford, UK). In order to achieve consistency between batches of colloid, quality control was performed by analysis of Raman spectra of each new batch of colloid. After the colloid preparation had been optimised, Raman spectra from 10 separate test batches of colloid were acquired in a quartz cuvette with a 100× objective lens, and 300 mW laser power. The average of these spectra was then used as a standard against which subsequent batches of colloid were compared. Batches deviating at any wave number by more than 5% from this ‘standard’ background were discarded. This quality control process prevented any spectral features due to impurities or inconsistencies in preparation affecting the SERS spectra and provided a consistent background spectrum for subtraction. The standard background spectrum is shown in Fig. 1. For accurate background subtraction, SERS spectra were baselined using the average spectra of the 10 colloidal test batches acquired with then same sample acquisition times as used for each SERS measurement.

Table 1
Peptide sequence and notation

Peptide sequence	Notation
H_2N–Cys–Lys–Ser–Ala–Lys–Ala–Thr–Lys–Ala–Tyr–Gln–Glu–Leu–OH	y
H_2N–Cys–Lys–Ser–Ala–Lys–Ala–Thr–Lys–Ala–Tyr(PO_3H_2)–Gln–Glu–Leu–OH	yP
H_2N–Cys–Lys–Ser–Ala–Lys–Ala–Thr–Lys–Ala–Ser–Gln–Glu–Leu–OH	s
H_2N–Cys–Lys–Ser–Ala–Lys–Ala–Thr–Lys–Ala–Ser(PO_3H_2)–Gln–Glu–Leu–OH	sP

Extinction spectra were obtained using an Ultraspec 430proUV/visible spectrophotometer (ULTRASPEC, Germany). Spectra of the colloid, both with and without the addition of the synthetic peptides, were acquired in a quartz cell over the wavelength range 250 to 1100 nm and referenced using pure water. The effect of peptide concentration upon colloid aggregation and hence SPR was investigated by obtaining extinction spectra as a function of peptide concentration over the range 0.1 nM to 1 μM.

Raman spectra were acquired using a Renishaw RM1000 Raman microscope (RENISHAW, Wooton-Under-Edge, UK) equipped with a 1200-line/mm grating providing a spectral resolution of 1 cm^{-1} and a diode laser providing excitation at 785 nm with up to 300 mW power. The system was calibrated using the Raman band of a silicon wafer at 520 cm^{-1}. Spectral data were acquired using Renishaw v.1.2 WiRE software coupled with GRAMS/AI (THERMO GALACTIC, USA).

The DCDR spectra were obtained by standard methods [12]. Briefly, a 5 μL volume of each 100 μM peptide solution was deposited on a DCDR substrate (TIENTA SCIENCE INC, USA) which, after drying for 30 min, formed a ring of approximately 1 mm in diameter. A 100× objective was used to focus on the ring and spectra collected using 300 mW laser power and a spectral integration time of 200 s over the range 1800 to 600 cm^{-1}.

SERS spectra were obtained by absorption of the analyte onto the colloidal surface; 100 μM peptide solutions were added to colloid, producing analyte concentrations of 100 nM. Peptide–colloid preparations were then incubated for 20 min at 25 °C before transferral to a 1536 well glass-bottomed Nanoplate with a well volume of 3 μl (EVOTEC TECHNOLOGIES, Germany). Spectra were acquired through the base of the well-plate using a 100× objective lens. To allow direct comparison with the DCDR spectra, SERS spectra of the pure peptide solutions were acquired over the same spectral range, 1800–600 cm^{-1}, with 300 mW laser power and a readout time of 10 s. To show that measurements could be performed on a time scale compatible with HTS, spectra of the 0 to 10% phosphorylated peptide mixtures were acquired using a ‘static grating scan’, which allowed rapid acquisition over a reduced spectral range. Scans covering 450 cm^{-1}, centred on 775 cm^{-1} were acquired with a total time of 1 second. Spectra were background corrected by subtracting the mean of the spectra obtained from the ‘naked’ colloid (Fig. 1).

Prior to interval partial least squares (iPLS) analysis, all spectra were preprocessed using a Savistky–Golay second derivative (SGSD) algorithm with a window width of 15 cm^{-1} which suppressed pixel noise without appreciably broadening any spectral features. The spectra were then mean centred and scaled to unity variance. Analysis was performed using an iPLS algorithm [36–38] (ITOOLBOX, Lars Nørgaard, Denmark) with five latent variables. The algorithm was trained with a representative group of spectra consisting of 20

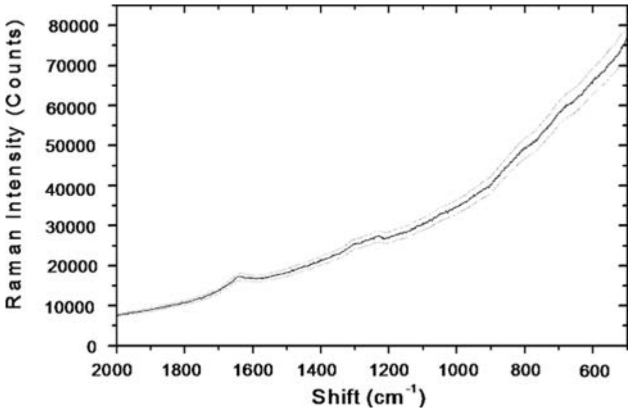

Fig. 1. The 'standard' colloidal background used to perform quality control of the colloids employed in this study. 5% deviation is indicated by the dashed lines.

independent measurements from each peptide composition using five different batches of colloid. The root mean standard error of prediction (RMSEP) in the predicted composition was determined using the leave-one-out method, in which each spectrum is used as a testing sample after training the algorithm with the remaining spectra. The iPLS interval was centred on the area containing the bands assigned to peptide phosphorylation and the interval width reduced until a minimum RMSEP was achieved and the greatest amount of variance captured with the least number of latent variables. Optimal intervals were found to be 900 cm^{-1} to 937 cm^{-1} for serine and 943 cm^{-1} 981 cm^{-1} for tyrosine. The iPLS interval served to eliminate the influence of less predicable spectral features, associated with changes in the secondary structure and colloid–peptide binding, upon the predicted values of peptide phosphorylation.

A complex chemical environment simulating a 'real' screening assay was prepared using bovine serum albumin (BSA), adenosine triphosphate (ATP) and adenosine diphosphate (ADP), purchased from SIGMA-ALDRICH (Poole, UK) with purity 98% or greater. A solution containing 15 mM BSA, 5 mM ADP and 5 mM ATP was added in equal volume to each 100 μM peptide mixture prior to 1:500 dilution in the colloid producing final concentrations of 15 μM BSA, 5 μM ADP, 5 μM ATP, and 100 nM peptide. Solutions were again transferred to a nanowell-plate for SERS analysis.

3. Results and discussion

Fig. 2 shows typical extinction spectra of the colloid prior to and 20 min after addition of synthetic peptide. The position of the 785 nm excitation is indicated by the vertical dashed line. Spectra obtained for all colloid batches used in this study did not exhibit deviation greater than the tolerance 5% indicated in Fig. 2. Prior to addition of the peptide, the colloid shows a sharp absorption peak at 400 nm with a tail to the long-wavelength side. Previous investigators [39] have attributed the sharp peak to surface plasmon resonance (SPR) on singular colloidal particles and the long-wavelength side-tail to SPR on aggregated particles [40–42]. Upon addition of the synthetic peptide the intensity of the side-tail increases into a broad peak, centred at 670 nm, with a greater intensity than the peak ascribed to the single particle SPR. Previous investigators [39] describe SERS as originating from plasmon resonances within this tail region. The change in extinction spectra was corroborated by an observed colour change from yellowish-brown to green. No noticeable difference in colloid extinction spectra was observed between the four peptides used, nor any of the peptide mixtures. The observed changes in plasmon resonance infer that the addition of the synthetic peptide causes the colloid to aggregate, possibly by modifying the surface charge. Previous investigations using colloidal SERS have reported that optimal enhancements are achieved from aggregated colloids [43–45]. Some investigators report adding aggregating agents such as sodium chloride to increase the effect.

The extinction spectra of the aggregated particles suggest that an assay of this type could be optimised by using a 670 nm excitation, however, the feature is sufficiently broad (full-width-half-maximum of 370 nm) to produce a substantial SERS signal at 785 nm. Monitoring the extinction spectra as a function of peptide concentration showed maximum aggregation at 100 nM with no further increase beyond this value. This value was used as the optimal peptide concentration for monolayer colloidal coverage [45].

The normalized DCDR spectra of the pure peptides (both phosphorylated and non-phosphorylated) are shown in Fig. 3. The assignments of the predominant Raman bands are as follows; 1667 cm^{-1} (amide I, C=O stretching, N–H deformation and C–N stretching), 1608 cm^{-1} (aromatic ring stretching of Tyr), ~1550 (Amide II backbone vibration), ~1440 cm^{-1} (CH_2 scissoring), ~1440–1460 (C–H_2 deformation), 1230 and 1222 cm^{-1} (amide III backbone vibration of the Serine and Tyrosine peptides respectively), 880 cm^{-1} (Ser), 842 and 822 cm^{-1} (Tyr doublet), 635 cm^{-1} (Tyr ring deformation). These band assignments agree with those of similar DCDR peptide studies performed by Xie et al. and Zhang et al. [13,15], small deviations are observed due to the differences in peptide sequence. Peaks at 742 (Ser) and 718 (Tyr), match unassigned peaks in earlier investigations by Zhang et al. [15]. We believe that these may be assigned to COO^- deformation vibrations [46]. Minor discrepancies in the positional band assignments between the two peptides used in this study and those reported by the previous investigators can be attributed to variation in peptide sequence.

The influence of the highly Raman active aromatic structure of the tyrosine side chain [15] causes phosphorylation of the

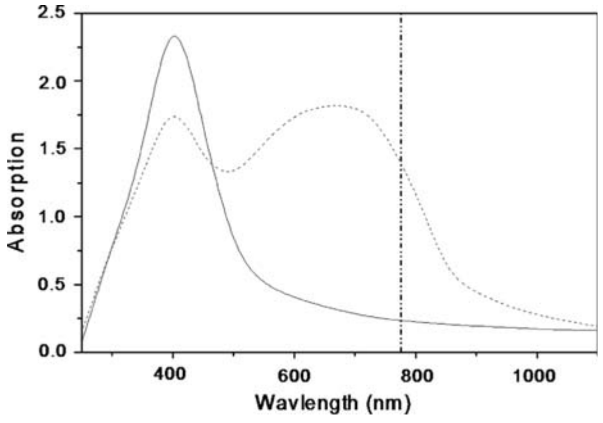

Fig. 2. Extinction spectra of the colloid both prior to (solid line) and several minutes after the addition of the synthetic peptide (S) at a concentration of 100 nM (dashed line). The position of the 785 nm excitation wavelength is denoted by the broken vertical line.

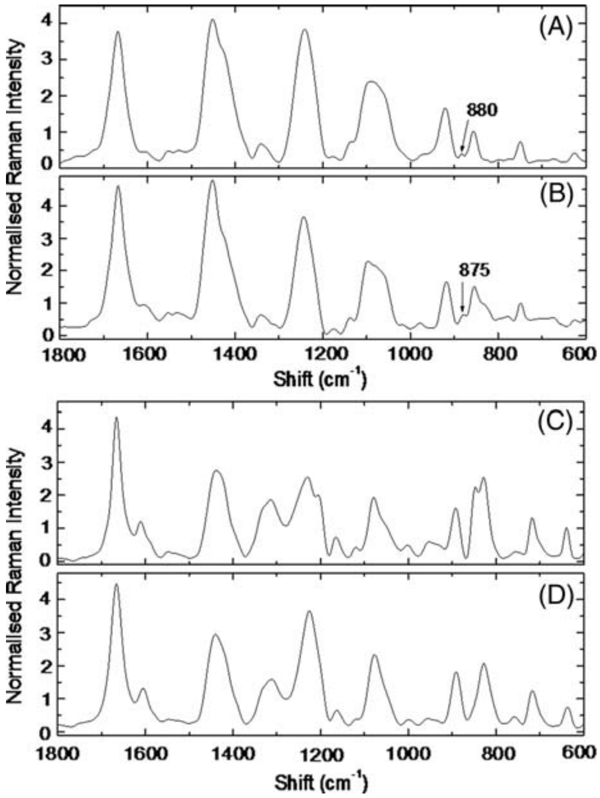

Fig. 3. Normalized DCDR spectra of the test peptides; (A) S (B) pS, (C) Y, (D) pY. The volume, 5 μL, and concentration, 100 μM, of the deposited solution are the same for all four solutions. A 100× objective was used and the spectra collected with a total integration time of 200 s, with a laser power of 300 mW.

tyrosine peptide to produce more appreciable spectral changes than those of the serine peptide. The most obvious feature being the tyrosine doublet at ∼830 cm^{-1} which collapses to a single band upon phosphorylation; this has previously been assigned to a Fermi resonance between symmetric ring-breathing of Tyr and an overtone of the out-of-plane ring vibration [13,47]. There is a decrease in vibrational frequency of the bands at 635 cm^{-1} and 1608 cm^{-1} to 631 cm^{-1} and 1600 cm^{-1} upon phosphorylation; this is attributed to the replacement of a hydrogen atom with a heavier phosphate group. There are also notable changes in the region associated with the amide III bands; the peak at 1222 cm^{-1} is down-shifted to 1216 cm^{-1} upon phosphorylation which indicates a conformational change. Furthermore, the shoulder at 1200 cm^{-1} (ring-C stretch Tyr) disappears upon phosphorylation which was also observed by Xie et al. [13].

Phosphorylation induced changes in the Raman spectra of the serine peptide are far more subtle than those of the tyrosine peptide, although none the less reproducible. The most significant difference between the non-phosphorylated and phosphorylated serine peptide spectra is the subtle shift of the 880 cm^{-1} serine band to 875 cm^{-1} which has also been observed previously [15]. There is also a subtle phosphorylation induced shift in the Raman band located at 626 cm^{-1} (assigned to COO^{-} wag vibrations [46]) to 624 cm^{-1}, which we have believed to arise from the addition of the heavier phosphate group.

The non-phosphorylated peptide spectra show differences in the positions of the amide III band, found at 1230 cm^{-1} for the serine peptide and 1222 cm^{-1} for the tyrosine peptide. This indicates that there are intrinsic differences in the secondary conformation of the two peptides due to the substitution of serine with the larger tyrosine. Furthermore, this band is down-shifted in frequency by 6 cm^{-1} in the case of the tyrosine peptide upon phosphorylation, indicating phosphorylation induced changes in secondary structure. Similar shifts are reported by previous investigators [15,13].

The SERS spectra of the pure peptide solutions are shown in Fig. 4. Although the majority of the enhanced bands show good positional correlation with the equivalent DCDR Raman data (Fig. 3), the relative intensities differ. It is known that SERS spectra show selective enhancements of bands due to bond orientation relative to the colloid surface. For this reason we shall only discuss the positions of SERS bands rather than their intensities which are less informative. The decrease in frequency of the serine band (880 to 875 cm^{-1}) upon phosphorylation is still visible, although slightly less pronounced due to broadening. The collapse of the tyrosine doublet at ∼830 cm^{-1} is clearly visible and again slightly broadened by the enhancement process. An intense mode at 1290 cm^{-1} appears in all four SERS spectra, but is not present in the DCDR spectra. This mode may arise from peptide–colloid interaction or from selective enhancement of a weak mode not visible in the

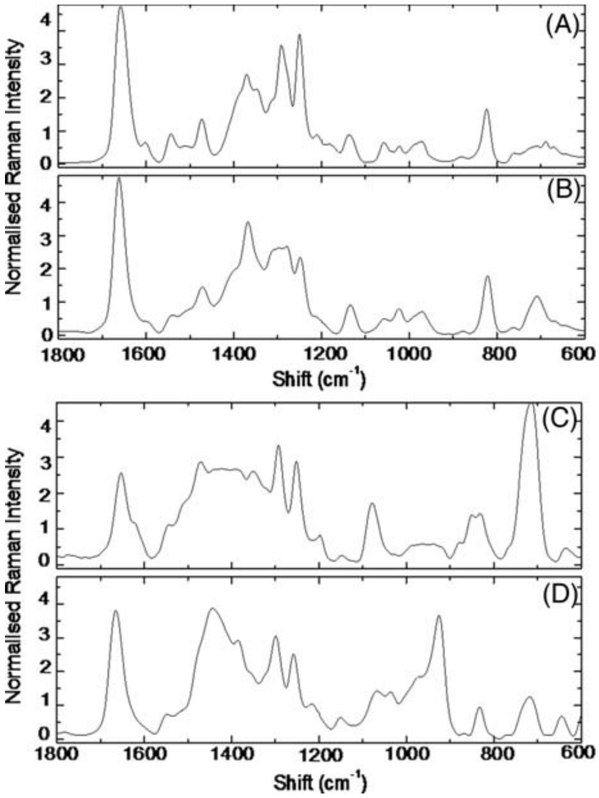

Fig. 4. Normalized SERS spectra of the test peptides; (A) S (B) pS, (C) Y, (D) pY. The volume, 3 μL, and peptide concentration, 100 nM, peptide/colloid conjugate is the same for all four peptides. A 100× objective was used and the spectra collected with a total integration time of 10 s, with a laser power of 300 mW.

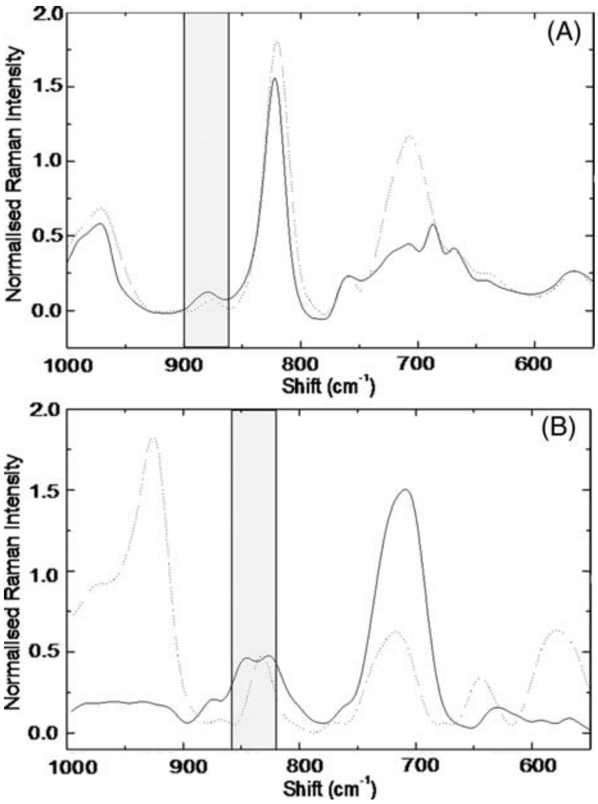

Fig. 5. Normalized SERS spectra over the reduced spectral ranges of the test peptides; (A) S (solid line) and pS (dashed line), (B) Y (solid line) and pY (dashed line). The volume, 3 μL, and peptide concentration, 100 nM, peptide/colloid conjugate is the same for all four peptides. A 100× objective was used and the spectra collected with a total integration time of 1 s, with a laser power of 300 mW. The shaded area indicates the iPLS interval used to predict the percentage of phosphorylated peptide.

DCDR spectra. Modes at 920 cm^{-1} (S and pS) and 890 cm^{-1} (Y and pY) are not present in the enhanced spectra, this may be due to selective enhancement of modes due to the orientation of the peptides on the colloidal surface.

There are other differences between the normal and enhanced spectra that depend upon peptide primary structure. The broad mode at 1080 cm^{-1}, present in all four DCDR spectra, is less pronounced in the enhanced spectra of the serine peptides, this mode is however present in the enhanced tyrosine spectra. The selective enhancement of this mode implies that replacing serine with a larger tyrosine residue may alter the orientation of the peptide on the colloidal surface, hence changing the relative enhancement of this mode.

The SERS spectra for both the serine and tyrosine peptides exhibit a shift in the position of the amide III bands when compared to their respective DCDR spectra; 1230 cm^{-1} to 1250 cm^{-1} and 1222 cm^{-1} to 1253 cm^{-1} respectively. This suggests that both peptides are in a different structural conformation when absorbed onto the colloidal surface than on the DCDR substrate. Unlike the DCDR spectra of tyrosine the SERS spectra showed no change in the amide band upon phosphorylation. This suggests that binding the tyrosine peptide to the colloidal surface may 'lock' its secondary structure which would otherwise change upon phosphorylation.

Fig. 5 shows the 'static-grating scans' acquired with an integration time of 1 second, for (A) peptides S and pS and (B) peptides y and pY. The spectra are centered on 775 cm^{-1} and span the region 1000–550 cm^{-1}. Other than differences in relative intensities, this region shows good positional correlation between the Raman bands of the phosphorylated and non-phosphorylated peptides. In Fig. 5A, the crucial difference between S and pS attributable to phosphorylation at the serine residue is the down-shift of the mode at 880 cm^{-1} to 875 cm^{-1}. The appearance of a larger mode, at 707 cm^{-1}, is attributed to changes in molecular orientation rather than phosphorylation due to lack of reproducibility in this feature. In Fig. 5B, the obvious effect of phosphorylation at the tyrosine residue is the collapse of the tyrosine doublet at 845 cm^{-1} and 825 cm^{-1} to a single mode at 830 cm^{1}. There is also a shift of the band at 628 cm^{-1} to 645 cm^{-1} and the bands at 594 cm^{-1} and 568 cm^{-1} form one large broad mode at 579 cm^{-1}. There is a significant variation in the intensity of the bands at 925 cm^{-1} and 972 cm^{-1} which may arise from selective enhancement of these modes caused by an alteration of the molecular orientation on the colloidal surface rather than a direct effect of phosphorylation at the tyrosine residue.

The predicted phosphorylation composition for the serine and tyrosine peptides was performed using the PLS algorithm with five latent variables. The captured variance was 91.0% and 93.2% and the root mean standard error of prediction (RMSEP) in percentage composition was 3.1 and 2.5 respectively. Fig. 6

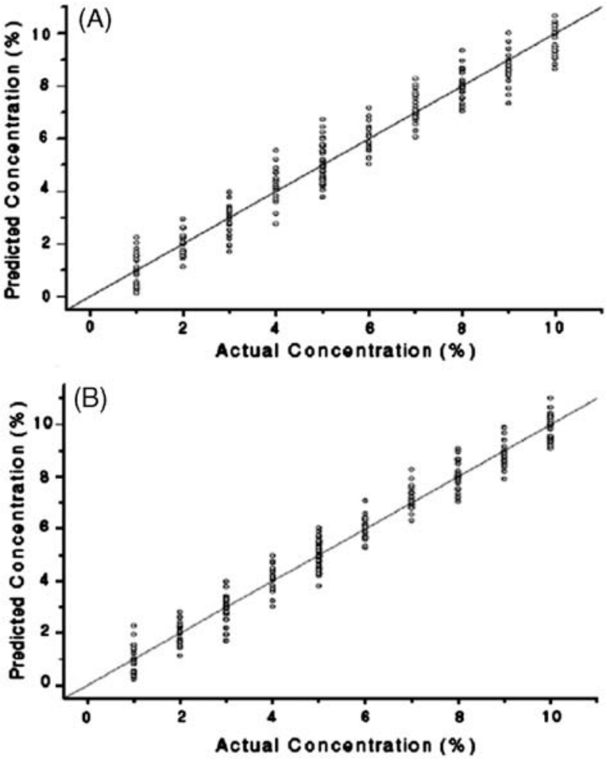

Fig. 6. iPLS-derived predictions of the percentage composition of phosphorylated vs. non-phosphorylated as a function of actual percentage composition for synthetic peptides (A) S and pS and (B) Y and pY. The straight line indicates a correlation of 100% between calculated and actual values. (R^2 = 0.94 and 0.96 respectively).

shows the resulting predicted percentages of phosphorylation plotted against the actual composition values for 20 independent readings of (a) mixtures of peptide S and pS and (b) peptides Y and pY. In both figures the straight line indicates perfect correlation between the predicted and actual peptide composition. The error in predicted composition for S and Y corresponding to *R*-squared values of 0.94 and 0.96 respectively.

The SERS spectra of the peptide solutions containing interfering compounds showed no obvious discrepancies from those acquired from the peptide/colloid solutions over the 450 cm^{-1} range covered by the 'static-grating scan'. Applying the iPLS algorithm, trained using the original spectra acquired from the non-complex peptide phosphorylation mixtures, to the spectra of the simulated assays produced predicted phosphorylation values which fell within the error limits generated from the measurements on the simple peptide mixtures.

Extinction spectra of the simulated assay solutions showed no noticeable deviation from those shown in Fig. 2. Furthermore, extinction spectra of the colloid with BSA and ADP/ATP alone shows no deviation from the 'naked' colloid, indicating that the interfering compounds do not induced aggregation, which infers a weak interaction with the colloid. This observation agrees with other investigator's [17] claims of the stability of silver colloid based SERS in BSA.

4. Conclusions

By using surface enhanced Raman scattering we have dramatically reduced the sampling time of Raman based detection of peptide phosphorylation at tyrosine and serine residues at physiologically relevant concentrations. Current Raman methods in this area rely upon DCDR to perform such measurements and require integration times of the orders of several hundred seconds; our proposed technique requires only one second, making SERS a feasible technique for near real-time detection applications, such as high-throughput screening.

The work presented shows that SERS can be used to detect peptide phosphorylation with a initial analyte concentration of 100 μM, on a par with DCDR. However, this is the analyte concentration prior to dilution into the colloidal solution; the optimal analyte concentration in the final solution required for monolayer coverage of the colloid was found to be 100 nM. Furthermore our results show that peptide phosphorylation could be detected with only 1 nM of phosphorylated peptide. With modification of the colloidal concentration it should be possible to achieve optimal monolayer coverage with initial analyte concentration in the sub-micromolar range.

We have shown that using multivariate analysis it is possible to quantify peptide phosphorylation with an error in the predicted phosphorylation of 3.1 and 2.5 percentage points at serine and tyrosine residues respectively. The difference in accuracy of the predicted phosphorylation for the peptide at serine and tyrosine residues can be attributed to the different spectral changes associated with phosphorylation of different amino acids. Phosphorylation at the tyrosine residue gives rise to a significant spectral change with the collapse of a doublet. Phosphorylation at the serine residue causes a far more subtle spectral change with a small positional shift of a single Raman band.

Results from a more complex mixture show that our technique can withstand interference from a complex protein (simulated using BSA) and other phosphorylated groups (simulated using ADP and ATP) that would be present in a real HTS assay. However, real assays solutions comprise of multiple diverse molecules that cannot be simulated by one protein alone. Therefore, individual assays, as with existing readout techniques, will require appropriate design, testing and optimisation depending upon the type of substrate and phosphorylating agents employed before they could be implemented into a HTS setting. Future work will focus upon applying this technique to a more realistic assay situation. For example, monitoring the effect of a known inhibitor compound via SERS titration of peptide phosphorylation with the addition of a phosphorylating agent.

When compared to the DCDR spectra, which were used to verify our band assignments, the SERS spectra showed both reliable and reproducible positional agreement. However, due to differential enhancement of vibrational modes depending upon their orientation to the colloidal surface, the amplitude of the bands was shown to be variable. For this reason we do not believe that SERS lends itself to detection of phosphorylation at theronine residues, which previous investigators have shown to solely produce changes in relative intensity rather than shifts in Raman bands.

The results from this study show that it is feasible to quantify peptide phosphorylation at specific sites using SERS. The proposed technique is complimentary to existing Raman based detection methods; due to the large signal enhancement it offers a vast reduction in detection times and the potential for lower concentration thresholds. Due to the variability in band amplitude SERS is limited to amino acid residues where phosphorylation induces changes in position. With this in mind, SERS is an ideal technique for applications such as high-throughput screen, where rapid measurement of a specific analyte is required.

References

[1] D. Foster, Intracellular signalling mediated by protein–tyrosine kinases: networking through phospholipid metabolism, Cell. Signal. 5 (1993) 389.

[2] J. Maller, On the importance of protein–phosphorylation in cell-cycle control, Mol. Cell. Biochem. 128 (1993) 267.

[3] T. Mustelin, P. Burn, Regulation of Src family tyrosine kinases in lymphocytes, Trends Biochem. Sci. 18 (1993) 215.

[4] P. Viatour, M.-P. Merville, V. Bours, A. Chariot, Phosphorylation of NF-[kappa]B and I [kappa]B proteins: implications in cancer and inflammation, Trends Biochem. Sci. 30 (2005) 43–52.

[5] S.K. Hanks, Genomic analysis of the eukaryotic protein kinase superfamily: a perspective, Genome Biol. 4 (2003) 111.

[6] J. Yan, N. Packer, A. Golley, K. Williams, Protein phosphorylation: technologies for the identification of phosphoamino acids, J. Chromatogr., A 808 (1998) 23–41.

[7] A.L. Jenkins, R.A. Larsen, T.B. Williams, Characterization of amino acids using Raman spectroscopy, Spectrochim. Acta, Part A: Mol. Biomol. Spectrosc. 61 (2005) 1585–1594.

[8] S.U. Sane, S.M. Cramer, T.M. Przybycien, A holistic approach to protein secondary structure characterization using amide I band Raman spectroscopy, Anal. Biochem. 269 (1999) 255–272.

[9] J. Thomas, P. Buzzini, G. Massonnet, B. Reedy, C. Roux, Raman spectroscopy and the forensic analysis of black/grey and blue cotton fibres: Part 1. Investigation of the effects of varying laser wavelength, Forensic Sci. Int. 152 (2005) 189–197.

[10] E.C.Y. Li-Chan, The applications of Raman spectroscopy in food science, Trends Food Sci. Technol. 7 (1996) 361–370.

[11] M. Pelletier, R. Altkorn, Raman sensitivity enhancement for aqueous protein samples using a liquid-core optical-fiber cell, Anal. Chem. 73 (2001) 1393–1397.

[12] D. Zhang, Y. Xie, C. Mrozek, C. Ortiz, V. Davisson, D. Ben-Amotz, Raman detection of proteomic analytes, Anal. Chem. 75 (2003) 5703–5709.

[13] Y. Xie, D. Zhang, G. Jarori, V. Davisson, D. Ben-Amotz, The Raman detection of peptide tyrosine phosphorylation, Anal. Biochem. 332 (2004) 116–121.

[14] C. Ortiz, D. Zhang, Y. Xie, V.J. Davisson, D. Ben-Amotz, Identification of insulin variants using Raman spectroscopy, Anal. Biochem. 332 (2004) 245–252.

[15] D. Zhang, C. Ortiz, Y. Xie, V.J. Davisson, D. Ben-Amotz, Detection of the site of phosphorylation in a peptide using Raman spectroscopy and partial least squares discriminant analysis, Spectrochim. Acta, Part A: Mol. Biomol. Spectrosc. 61 (2005) 471–475.

[16] P.D. O'Neal, G. Cote, M. Motamedi, J. Chen, W. Lin, Feasibility study using surface-enhanced Raman spectroscopy for the quantitative detection of excitatory amino acids, J. Biomed. Opt. 8 (2003) 33–39.

[17] K. Kneipp, Y. Wang, R.R. Dasari, M.S. Feld, Near-infrared surface-enhanced Raman scattering (NIR-SERS) of neurotransmitters in colloidal silver solutions, Spectrochim. Acta, Part A: Mol. Biomol. Spectrosc. 51 (1995) 481–487.

[18] N. Isola, D. Stokes, T. Vo-Dinh, Surface-enhanced Raman gene probe for HIV detection, Anal. Chem. 70 (1998) 1352–1356.

[19] T. Vo-Dinh, D. Stokes, G. Griffin, M. Volkan, U. Kim, M. Simon, Surface-enhanced Raman scattering (SERS) method and instrumentation for genomics and biomedical analysis, J. Raman Spectrosc. 30 (1999) 785–793.

[20] K. Kneipp, A. Haka, H. Kneipp, K. Badizadegan, N. Yoshizawa, C. Boone, K. Shafer-Peltier, J. Motz, R. Dasari, M. Feld, Surface-enhanced Raman spectroscopy in single living cells using gold nanoparticles, Appl. Spectrosc. 56 (2002) 150–154.

[21] J. Creighton, C. Blatchford, M. Albrecht, Plasma resonance enhancement of Raman scattering by pyridine adsorbed on silver or gold sol particles of size comparable to the excitation wavelength, J. Chem. Soc., Faraday Trans. II 75 (1979) 789–790.

[22] J.V. Garcia-Ramos, S. Sanchez-Cortes, Metal colloids employed in the SERS of biomolecules: activation when exciting in the visible and near-infrared regions, J. Mol. Struct. 405 (1997) 13–28.

[23] M.E. Uppitsch, Observation of surface enhanced Raman spectra by adsorption to silver colloids, Chem. Phys. Lett. 74 (1980) 125–127.

[24] H. Xu, C.-H. Tseng, T.J. Vickers, C.K. Mann, J.B. Schlenoff, Near-infrared surface-enhanced Raman spectroscopy of chemisorbed compounds on gold colloids, Surf. Sci. 311 (1994) L707–L711.

[25] F. Wang, J. Zheng, X. Li, Y. Ji, Y. Gao, W. Xing, T. Lu, Surface-enhanced Raman spectroscopy of microperoxidase-11 on roughed silver electrodes, J. Electroanal. Chem. 545 (2003) 123–128.

[26] V.H. Wysocki, K.A. Resing, Q. Zhang, G. Cheng, Mass spectrometry of peptides and proteins, Methods 35 (2005) 211–222.

[27] M. Graff, J. Bukowska, K. Zawada, Surface enhanced Raman scattering (SERS) of 1-hydroxybenzotriazole adsorbed on a copper electrode surface, J. Electroanal. Chem. 567 (2004) 297–303.

[28] Z. Liu, G. Wu, Surface-enhanced Raman scattering of thiourea adsorbed on the silver electrode: bond polarizability derivatives as elucidated from the Raman intensities, Chem. Phys. Lett. 389 (2004) 298–302.

[29] A. Wei, B. Kim, B. Sadtler, S. Tripp, Tuneable surface-enhanced Raman scattering from large gold arrays, ChemPhysChem 12 (2001) 743–745.

[30] N. Felidj, J. Aubard, G. Levi, Optimised surface-enhanced Raman scattering on gold nanoparticle arrays, Appl. Phys. Lett. 82 (2003) 3095–3097.

[31] N. Felidj, J. Aubard, G. Levi, Controlling the optical response of regular arrays of gold particles for surface-enhanced Raman scattering, Phys. Rev., B 65 (2002) 075419.

[32] D.L. Stokes, T. Vo-Dinh, Development of an integrated single-fiber SERS sensor, Sens. Actuators, B, Chem. 69 (2000) 28–36.

[33] C. Viets, W. Hill, Single-fibre surface-enhanced Raman sensors with angled tips, J. Raman Spectrosc. 31 (2000) 625.

[34] C. Viets, W. Hill, Fibre-optic SERS sensors with conically etched tips, J. Mol. Struct. 563 (2001) 163–166.

[35] V.A. Markel, Near-field optical spectroscopy of individual surface-plasmon modes in colloid clusters, Phys. Rev., B 59 (1999) 10903.

[36] L. Norgaard, A. Saudland, J. Wagner, J.P. Nielsen, L. Munck, S.B. Engelsen, Interval partial least-squares regression (iPLS): a comparative chemometric study with an example from near-infrared spectroscopy, Appl. Spectrosc. 54 (2000) 413–419.

[37] A. Borin, R.J. Poppi, Application of mid infrared spectroscopy and iPLS for the quantification of contaminants in lubricating oil, Vibr. Spectrosc. 37 (2005) 27–32.

[38] S. Navea, R. Tauler, A.D. Juan, Application of the local regression method interval partial least-squares to the elucidation of protein secondary structure, Anal. Biochem. 336 (2005) 231–242.

[39] S. Hayashi, R. Koga, M. Ohtuji, K. Yamamoto, M. Fujii, Surface-plasmon resonances in gas-evaporated Ag small particles—effects of aggregation, Solid State Commun. 76 (1990) 1067–1070.

[40] C.G. Blatchford, J.R. Campbell, J.A. Creighton, Plasma resonance-enhanced Raman scattering by adsorbates on gold colloids: the effects of aggregation, Surf. Sci. Lett. 120 (1982) A339.

[41] J. Chowdhury, M. Ghosh, Concentration-dependent surface-enhanced Raman scattering of 2-benzoylpyridine adsorbed on colloidal silver particles, J. Colloid Interface Sci. 277 (2004) 121–127.

[42] Y. Du, Y. Fang, Assignment of charge transfer absorption band in optical absorption spectra of the adsorbate-silver colloid system, Spectrochim. Acta, Part A: Mol. Biomol. Spectrosc. 60 (2004) 535–539.

[43] T. Tanaka, A. Nakajima, A. Watanabe, T. Ohno, Y. Ozaki, Surface-enhanced Raman scattering spectroscopy and density functional theory calculation studies on adsorption of o-, m-, and p-nitroaniline on silver and gold colloid, J. Mol. Struct. 661–662 (2003) 437–449.

[44] M.S. Kim, J.S. Kang, S.B. Park, M.S. Lee, Surface-enhanced Raman spectroscopy of quinomethionate adsorbed on silver colloids, Bull. Korean Chem. Soc. 24 (2003) 633–637.

[45] K. Faulds, R.E. Littleford, D. Graham, G. Dent, W.E. Smith, Comparison of surface-enhanced resonance Raman scattering from unaggregated and aggregated nanoparticles, Anal. Chem. 76 (2004) 592–598.

[46] S. Stewart, P.M. Fredericks, Surface-enhanced Raman spectroscopy of peptides and proteins adsorbed on an electrochemically prepared silver surface, Spectrochim. Acta, Part A: Mol. Biomol. Spectrosc. 55 (1999) 1615–1640.

[47] M.N. Siamwiza, R.C. Lord, M.C. Chen, T. Takamatsu, I. Harada, H. Matsuur, T. Shimanouchi, Interpretation of the doublet at 850 and 830 cm^{-1} in the Raman spectra of tyrosyl residues in proteins and certain model compounds, Biochemistry 14 (1975) 4870–4876.